Evaluation of Delamination Damage on Composite Plates using an Artificial Neural Network for the Radiographic Image Analysis

Victor Hugo C. de Albuquerque[1], João Manuel R. S. Tavares[2], Luís M. P. Durão[3]

[1]Instituto de Engenharia Mecânica e Gestão Industrial (INEGI), Faculdade de Engenharia da Universidade do Porto (FEUP), Rua Dr. Roberto Frias, s/n, 4200-465 PORTO, PORTUGAL

email: victor.albuquerque@fe.up.pt

[2]Instituto de Engenharia Mecânica e Gestão Industrial (INEGI), Faculdade de Engenharia da Universidade do Porto (FEUP), Departamento de Engenharia Mecânica (DEMec), Rua Dr. Roberto Frias s/n, 4200-465 PORTO, PORTUGAL

email: tavares@fe.up.pt, url: www.fe.up.pt/~tavares

[3]Centro de Investigação e Desenvolvimento em Engenharia Mecânica (CIDEM), Departamento de Engenharia Mecânica (DEM), Instituto Superior de Engenharia do Porto (ISEP), R. Dr. António Bernardino de Almeida nº 431, 4200-072 PORTO, PORTUGAL

email: lmd@eu.ipp.pt

Corresponding author:

Prof. João Manuel R. S. Tavares
Faculdade de Engenharia da Universidade do Porto (FEUP)
Departamento de Engenharia Mecânica (DEMec)
Rua Dr. Roberto Frias, s/n
4200-465 PORTO
PORTUGAL
Telf.: +315 22 5081487, Fax: +315 22 5081445
Email: tavares@fe.up.pt Url: www.fe.up.pt/~tavares

Abstract

Drilling carbon/epoxy laminates is a common operation in manufacturing and assembly. However, it is necessary to adapt the drilling operations to the drilling tools correctly to avoid the high risk of delamination. Delamination can severely affect the mechanical properties of the parts produced. Production of high quality holes with minimal damage is a key challenge. In this paper, delamination caused in laminate plates by drilling is evaluated from radiographic images. To accomplish this goal, a novel solution based on an artificial neural network is employed in the analysis of the radiographic images.

Keywords: Drilling, Image Segmentation, Image Analysis, Maximum Thrust Force, Delamination Factors, Non-destructive Testing

1 Introduction

Over the past decades, fibre reinforced plastics have become more important due to their unique properties such as low weight, high strength and stiffness. Although earlier developments of such materials were mostly dedicated to the aerospace and aeronautical industries, recent years have seen a rapid spread of their use in many other industries such as automotive, railway, naval and sports. Concerns of their high costs have been satisfactorily addressed by adopting high volume production and innovative design. In spite of these advances, their use is still limited, mainly due to the high cost usually associated to their machining and finishing operations. Although composite components are usually produced to near-net shape, machining is often needed to comply with dimensional and geometrical tolerances or assembly needs. For these materials, machining operations can be carried out using conventional machinery with the adequate adaptations. Drilling is one of the commonest machining processes used on composite materials for making holes for screws, rivets and bolts. Since composite materials are neither homogeneous nor isotropic, the drilling of these materials can lead to damages in the regions around the drilled holes. The most frequent defects caused by drilling composite materials are delamination, fibre pull-out, interlaminar cracks or thermal degradation [1].

These machining defects not only cause a reduced load carrying capacity of the laminate [2], but also affect its reliability [3]. Both outcomes are undesired, although considered a normal consequence of drilling in composite materials. In addition, a high rate of tool wear is usually associated with machining fibre reinforced plastic laminates, due to the high abrasiveness of the reinforcing fibre. This in turn increases the total operation time, due to frequent tool replacement. Consequently there is a need for good

quality holes in composite materials, which requires knowledge of the materials, operations and tools involved.

Drilling is a complex process characterized by extrusion and cut mechanisms. The former is realized by the drill chisel edge that has null or very low linear speed and the later is realized by the existence of rotating cutting lips at a certain speed.

Several approaches have been presented to reduce delamination in composite plates, universally considered as the most serious damage during drilling. For example, Piquet et al. [4] carried out an experimental analysis of drilling damage in thin carbon/epoxy plates using special drills. These authors concluded that the use of a small rake angle, a significant number of cutting edges and a point angle of 118º for the main cutting edges can reduce the damage incurred. Also, reduced chisel edge dimensions can prevent delamination onset. Palanikumar et al. [5] analyzed the influence of drill point angles in high speed drilling. The authors stated that the effect of drilling parameters on delamination is independent of the drill point angle used. In a study carried out by Persson et al. [6] the effect of machining defects on the strength and fatigue life of composite laminates is discussed. The authors proposed a different method for generating holes by combining the axial and radial movements of the tool used. This patented method eliminates the stationary tool centre which reduces the axial thrust force. Additionally, it also reduces the risk of tool clogging. A series of machining experiments was conducted by Dharan and Won [7] who proposed an intelligent machining scheme to prevent delamination in composite materials. The technique was to limit the feed during the critical step of the machining process so as to reduce the risk of delamination. In another work Hocheng et al. [8] concluded that a range of cutting parameters for optimization should be defined. Both feed rate and

cutting speed should be conservative, since an increase in the feed rate can cause delamination and burrs, while an increase in the cutting speed raises the thrust force and torque and consequently reduces the tool life.

Murphy et al. [9] studied the performance of three different types of carbide drills, either uncoated or with TiN or DLC (diamond like carbon) coating. Their results indicated that coated drills did not reduce tool wear or damage when drilling carbon reinforced laminates. However, in comparison to high speed tools, the carbide tools with or without coatings presented superior wear resistance.

Won and Dharan [10] established the contribution of chisel edge cutting force in the total thrust force. The chisel edge force was always 60 to 85 % of the total force, independently of the hole diameter. This contribution is more relevant if higher feed rates are used when drilling. In another work by the same authors [11], the effect of chisel edge and pilot hole on thrust force was also studied. They observed that an increase in feed rate has an important influence on the chisel edge effect, while an increase of tool diameter decreases this effect. Delamination is mainly caused by the thrust force acting on the chisel edge. Tsao and Hocheng [12] studied the effect of chisel edge length on delamination onset and a thrust force reduction of 20 to 25 % was found when a pilot hole was used. According to this work, the dimensionless chisel edge length should be around 0.09 to 0.2 of the drill diameter. This gives an indication of the dimension of a pilot hole to reduce the delamination risk in the drilling of composite laminates. Adopting a two stage drilling strategy, the diameter of the pilot hole should be equal to the length of the chisel edge used in the final drill and a ratio of 0.18 between the diameters of the pilot hole and the final drill was suggested. The effect of the pilot hole diameter on delamination of core drills was analyzed by Tsao [13].

According to this work, a suitable control of the ratio between the diameters of the pilot hole and the final drill can allow higher feed rates without causing delamination. Despite these problems, the use of composite plates is growing incessantly in many areas. Therefore, with this production increase in composite parts the design of high quality machining setups based on optimized cutting parameters and specific tools are urgently required.

As some of the defects in the laminate plates caused by drilling operations cannot be correctly identified only by visual inspection, suitable non-destructive testing procedures should to be set up to determine the existence of any internal damages between the laminate plies. Moreover, as the carbon/epoxy laminate plates are opaque, enhanced radiography or other suitable imaging modalities, should be employed for plate damage evaluation [14, 15].

In the present work, delamination associated to the drilling of composite plates using different tools and diverse feed rates was evaluated considering two delamination factors based on data acquired from radiographic images. To do this a novel approach based on a backpropagation neural network was employed to analyze the images used. This new approach accomplished a robust characterization of the delaminated regions from the radiographic images used, overcoming some of the problems usually associated with such images, like high noise levels, low contrast and pixels intensity variation [14, 15]. Additionally, the results of delamination are compared with the thrust forces involved with the purpose of enhancing the importance of thrust force reduction in delamination minimization.

This paper is organized as follows: In the next section, the theoretical background of the methodologies used is presented; thus, the damage models and criteria, tasks of

image processing and analysis and the artificial neural network employed are introduced. In the third section, the experimental work is outlined. The results and their discussion are presented in section four and finally in the last section, the main conclusions are presented.

2 Theoretical Background

2.1 Damage Models for Delamination in Composite Materials

To carry out a detailed analysis on the delamination process in composite materials, two main classes should be considered, according to their causes and consequences: one is commonly known as peel-up delamination and the other as push-down delamination.

Peel-up delamination is caused by the cutting force pushing the abraded and cut material to the flute surface, Figure 1a. At first contact, the cutting edge of the drill will abrade the laminate. As the drill moves forward, it tends to pull the abraded material along the flute, making the material spiral up before being effectively cut. Then, a peeling force pointing upwards is introduced that tends to separate the upper laminas of the uncut portion held by the downward acting thrust force. Usually, a reduction in the feed rate can decrease this effect.

The second delamination class, usually designated as push-down delamination, occurs in the interlaminar regions, so it depends not only on the nature of the fibre but also on the resin type and its properties. This damage is a consequence of the compressive thrust force that the drill tip always exerts on the uncut plies of the workpiece. At some point, the load exceeds the interlaminar bond strength and delamination occurs, before the laminate is totally penetrated by the drill, Figure 1b. This damage is especially difficult to detect by visual inspection and severely reduces

the load carrying capacity of the laminate part, particularly under compression loading [2].

Analyses of delamination mechanisms during drilling using a Linear Elastic Fracture Mechanics approach have been developed and different models proposed. The contribution of the thrust force in delamination onset and propagation was first demonstrated by Hocheng and Dharan [16], who developed a model based on Fracture Mechanics to determine the critical thrust force for delamination. This important analytical delamination model, which establishes the critical thrust force for the onset of delamination (F_{crit}), is related to the material and the geometrical properties of the unidirectional laminate, such as the elastic modulus (E_1), the Poisson ratio (ν_{12}), the interlaminar fracture toughness in mode I (G_{Ic}) and the uncut plate thickness (h):

$$F_{crit} = \Pi \left[\frac{8 G_{Ic} E_1 h^3}{3(1-\nu_{12}{}^2)} \right]^{1/2} . \qquad (1)$$

Besides the Hocheng-Dharan model, other models have been presented to determine the thrust force for delamination onset and propagation, see [17-19]. Recent models use a different approach, based on specific drill geometry [20] or in a comparison of geometries using Taguchi techniques [21] or the influence of the stacking sequence [22]. In each case, a different model for the estimation of the critical thrust force for delamination onset is derived.

2.2 Damage Criteria for Delamination in Composite Materials

Criteria for comparison and evaluation of delamination damages have to be established. Damaged extension can be evaluated through nondestructive tests such as ultrasonic, acoustic emission, radiography, C-Scan or computerized tomography (CT) in order to

acquire images of the hole and surrounding areas for further analysis, examples of such works are described in [23-27]. Additionally, several delamination factors have been proposed.

Chen [28] proposed a comparison factor that enables the evaluation and analysis of the delamination extension in composite materials. The proposed Delamination Factor (F_d), is defined as the ratio between the maximum delaminated diameter D_{max} and the nominal hole diameter D , according to:

$$F_d = \frac{D_{max}}{D}. \tag{2}$$

An original approach was accomplished by Davim et al. [29] by proposing another criterion, named Adjusted Delamination Factor (F_{da}). This new criterion is intended to deal with the irregular form of delamination containing breaks and cracks and it is defined as a sum of two contributions:

$$F_{da} = \alpha \frac{D_{max}}{D_o} + \beta \frac{A_{max}}{A_o}, \tag{3}$$

where the first quotient is the delamination factor given by Eq. 2 multiplied by a constant α ; A_{max} is the area related to the maximum diameter of the delamination zone (D_{max}) and A_o is the area of the nominal hole (D_o). Constants α and β are weights, with their sum being equal to 1 (one).

These damage evaluation criteria are based on the existence of measurements obtained from the damaged regions. Thus, it is important to acquire clear images of these regions that can then be analyzed using suitable techniques for image processing and analysis.

2.3 Image Processing and Analysis

Image processing and analysis is an important scientific research field for acquiring images, enhancing their quality and contents and extracting high level information from them, see [30, 31].

The first task in image processing and analysis is concerned with the acquisition of the images. This can be accomplished by using off the shelf digital cameras, microscopy imaging devices or X-ray imaging devices. This latter solution was used in this work to obtain the images that would be further analyzed to evaluate the delamination damages involved.

After the acquisition step there is a processing step that basically uses image processing techniques to enhance the original images by noise removal, geometrical correction, edges or regions enhancement, see, for example, [30, 31]. This step is crucial for the success of the following steps and for the many applications of image processing and analysis. Frequently, the following step of a common system of image processing and analysis is image segmentation.

Image segmentation process divides the input image into regions according to their properties. The success of the image segmentation step is very important as the image analysis step, which follows, is expected to obtain robust and reliable descriptors and measurements from the segmented regions [32]. Generally the type of image segmentation used depends on the application involved [31, 32]. There are several approaches to carry out image segmentation, such as those based on deformable models, statistical modeling, physical modeling, deformable templates and neural networks, see [30, 31, 33-36].

The descriptors and measurements obtained from the image analysis step can also

be used as attributes to a following processing task, usually known as Pattern Recognition, in which strategies to recognize the regions analyzed are employed, see [31].

In the authors' previous works, the images with the damaged areas were analyzed using manual techniques of image processing and analysis; in particularly, by employing techniques of noise smoothing, image segmentation, morphologic image enhancement and analysis of regions that were already integrated in a previously built computational platform, see [14, 15, 37]. However, in this work the same regions were segmented from the input radiographic images using a novel approach based on an artificial neural network. After the training phase of the network, this new approach automatically segments the input images, improving its robustness, flexibility, accuracy and efficiency. The artificial neural network used here was designed and integrated to a new computational system, especially developed to analyze the kind of images considered in this work.

2.4 Artificial Neural Network

Artificial neural networks can be successfully applied in problems of function approximation and classification, among others, even when there are nonlinear relations between the dependent and independent variables.

Artificial neural networks are being used in Material Sciences for welding control [38], to define relations between parameters and correlations in Charpy impact tests [38], in the modeling of alloy elements [39, 40], in the prediction of welding parameters in pipeline welding [41], in modeling the microstructures and mechanical properties of steels [42], in modeling the deformation mechanism of titanium alloys in hot forming

[43], for the prediction of properties of austempered ductile irons [44], for the prediction of the carbon contents and the grain sizes of carbon steels [45], in building models to predict the flow stress and microstructure evolution of hydrogenised titanium alloys [46], in microstructure segmentation and quantification [33, 34], and so on..

Because of their high robustness to the presence of noisy data in the input images, execution speed and their likelihood for being parallelly implemented, many image processing and analysis systems have been developed based on artificial neural networks, see [33, 34, 47].

The fundamental paradigm of neural networks is to construct a composed model using a considerable number of units, known as neurons that constitute very simple processing units, with a great number of connections between them. The information among the neurons employed in the network is transmitted through the associated synaptic weights.

The flexibility of the artificial neural networks as well as their capacity to learn and to generalize the learned information are very attractive and important aspects that justify their wide use. In fact, the capability for generalization, associated with the capacity to learn through a training set, representative of the problem involved and then the ability to provide correct results to input data that was not presented in the training set, demonstrates their excellent proficiency. Additionally, artificial neural networks can extract information not presented in explicit forms in the training sets used [48].

Different topologies and algorithms for neural networks have been proposed in function of the application involved. In this work, a multilayer perceptron neural network of the feedforward type was used [33, 34, 49].

Usually, a multilayer perceptron network is composed of several layers lined with

neurons. The input data is presented to the first layer, which distributes it through the internal hidden layers. The last layer is the output layer of the neural network from which is obtained the solution to the problem. The input layer and the output layer can be separated by one or more hidden layers, also called intermediate layers, but in many applications just one hidden layer is used. The neurons of a layer are connected to the neighboring neurons and there are no unidirectional communications or connections among the neurons of the same layer [33, 34, 48, 49].

In this work, the segmentation of the radiographic images for evaluation was accomplished using a novel approach of image segmentation based on a neural network that identifies the pixels of the input images belonging to the drilled hole, damaged and non-damaged areas. The topology of the adopted neural network consists of a three layer multilayer perceptron network, made up of three inputs, two perceptrons in the hidden layer and three perceptrons in the output layer, Figure 2. On one hand, the number of inputs of the adopted topology was defined in function of the inputs to be presented to the neural network: the color components R, G and B, that is, the components red, green and blue of the pixels of the image to be evaluated. On the other hand, the number of outputs was defined in function of the classification classes of the pixels being analyzed: drilled hole, damaged or non-damaged areas. Additionally, the number of neutrons integrated in the hidden layer was defined using the approach proposed in [50]. The training of the neural network was carried out using the backpropagation algorithm, which is the classical training solution for this neuronal network architecture [33, 34, 49]. In this training step that needs to be performed just once for equivalent image sets, sets of representative pixels of each classification class are inputted into the network with the identification of the associated class.

The main reason to select the topology described for the neural network adopted here was its excellent performance in the segmentation of material microstructures from metallographic images, see [33, 34] that have segmentation problems very similar to the ones involved in this work. However, different neural network topologies could be used to accomplish the segmentation task involved in this work, but probably with higher computational costs and complexity.

2.5 Experimental Procedure

In this section, the experimental steps taken to evaluate, from radiographic images, the delamination damages caused in composite plate samples by drilling operations using different tools and diverse feed rates is described, Figure 3.

2.5.1 Tools and drilling methods

In order to perform the desired experimental analysis, a carbon/epoxy plate was fabricated from pre-preg with a stacking sequence of $[(0/-45/90/45)]_{4s}$, providing quasi-isotropic properties to the plate. The pre-preg used was TEXIPREG® HS 160 REM, from SEAL. The laminate was cured for one hour in a hot plate press, under 3 kPa pressure and 140 ºC, followed by air cooling, as indicated by the manufacturer. The final the plate thickness was 4 mm. From these plates, five test coupons of 135x35 mm for each test batch were cut, resulting in a total of fifty test coupons.

Drilling experiments were performed on an OKUMA MC-40VA machining centre, Figure 4 and all drills used were made of K20 carbide and have a diameter of 6 mm. As one of the aims of this work was to evaluate the damage caused by diverse drill geometries, the experiments were performed under the worst practical conditions; that

is, without reinforcement plates either under or above the plate to be drilled. The plate located below the test plate is usually known as “sacrificial plate”.

A collection of four different standard helical drills was used: twist with 118º point angle, twist with 85º point angle, ‘Brad’ type and four flute, Figure 5. The most commonly used drill is the twist drill with a 118º point angle, which is available in all manufacturers’ catalogues and is well adapted for metal drilling. Its convenience for composite materials is one of the outcomes expected from this work. An alternative twist drill is the 85º point angle, with a construction similar to the first one except for the point angle, which was used to evaluate the importance of a sharper tool point in the thrust force and delamination. The Brad drill used was originally developed for wood cutting. Its main characteristic is the scythe shape of the cutting edges, tensioning the fibers in order to obtain a clean cut and a smooth machined surface. The use of four-flute drills, already suggested in [4], has the advantage of reducing the heat build-up, by reducing the contact time between each cutting edge with the material, which allows the use of higher feeds or speeds without the risk of delamination. This has an important effect on productivity that represents a substantial advantage for commercial tools.

A cutting speed of 53 m/min, corresponding to a spindle speed of 2800 rpm and two feed rates of 0.06 and 0.12 mm/rev were used. Thus, the differences involved in the tests performed are related to the drill geometry and feed rate, allowing an assessment of these two effects. For a more comprehensive evaluation of feed rate effects, a third feed rate of 0.02 mm/rev was used with the twist drills. The selection of the spindle speed and feed rates was based on the authors’ previous experience [14, 15], as well as on the usual parameters found in related literature and also from the manufacturers’ recommendations, besides the required homogenization of the parameters considered

for an adequate comparison.

2.5.2 Thrust force monitoring

During the drilling operations, the thrust force was continuously monitored by a Kistler 4782 dynamometer and its signal was transmitted via an amplifier to a personal computer (PC). For each cutting condition, drill and cutting parameters, a total of six holes were made in a test coupon and the thrust force was always averaged over one spindle revolution, in order to reduce signal variation that inevitably occurs. The robustness of the results was checked using statistical tools, like standard variation and repetition of the experimental steps when necessary. Results presenting large variations were ignored and the procedures repeated.

2.5.3 Use of damage analysis techniques

Internal delamination extensions cannot be analyzed by visual inspection since carbon/epoxy plates are opaque. However, as already discussed in section 2.2, there are several imaging modalities that can be used to acquire images, like radiography, C-Scan or CT that can be computationally processed in order to evaluate the delamination extension.

Compared with radiography, C-Scan needs a longer time to acquire the images because of its higher resolution and the low speed of its test probe and TC installations are rather expensive for now. Furthermore, the usual setup time of a C-Scan device is longer and, as in the authors' case, the accessibility of these devices is often reduced. However, radiography is suitable for the detection of delamination damages only if a contrasting fluid is used. The fluid used was di-iodomethane, a radio-opaque chemical

reagent. Thus, the sample plates were immersed for one and a half hours and then radiographic images were acquired adopting an exposition time of 0.25 seconds. This process is simple and allows the acquisition of several plates simultaneously, independently of their thickness.

2.5.4 Artificial Neural Network

The images acquired by radiography show dark grey areas corresponding to damaged regions and light grey areas to undamaged regions of the plates and the delaminated areas were located in a relatively circular region around the drilled holes, Figure 6.

To accomplish the segmentation of the drilled hole and damage areas in the acquired images, the adopted neural network was trained by selecting, from some training images, several sample pixels of each area to be segmented and indicating the associated area. The number of training images and the number of sample pixels for each area was defined from experimental tests in order to accomplish a good compromise between user effort and the quality of the output results. Thus six training images and an average of ten sample pixels for each area and per each training image were used. It should be noted that the training of the network needs to be done only once for analogous input image sets; although, different numbers of training images and sample points could be used leading to successful segmentation results as well.

After the network training, the acquired images were segmented and then the resultant images were processed using the region growing technique [31], in order to merge some regions that appeared split but should be combined and finally the desired measurements were obtained by scanning the associated areas to find the desired

measured points, Figure 7. As can be seen in this Figure, despite the high complexity of the original image, the novel segmentation approach obtained good results, which would be very difficult to accomplish using the more traditional image segmentation methods, such as image binarization by threshold value.

3 Experimental Results and Discussion

In this section, the experimental results are presented and discussed. The results concerning the thrust force and delamination due to the drill geometry and feed rate used are shown and analyzed.

3.1 Thrust Force

The results for the thrust force (F_x) are the average of six tests under identical experimental conditions. Since delamination onset and propagation depend largely on the maximum value of the thrust force, this value is regarded as the most suitable for comparison.

As previously stated, for each parameter setting on a test coupon, a total of six holes was drilled, so all results are an average of six individual tests. For reasons of clarity, only the final average for each drill and setting is presented.

3.1.1 Drill geometry effect

The thrust force results in Figure 8 show that the lowest thrust force value was obtained when the 85º point angle twist drill was used. However, for higher feed rates the thrust force value became similar to those observed with the Brad drill machining. When the 118º angle twist drill was used, the thrust force values increased by

approximately 20%, which can be explained by the larger chisel edge of this drill in comparison to the 85º angle drill. The consequence of a larger point angle is an enlargement of the area responsible for the extrusion effect on the uncut plies of the laminate and consequently a higher thrust force. The highest thrust force value was found when the four flute drill was used, for both feed rates considered in the experimental work. In fact, the maximum thrust force value almost doubles the associated value of the 85º point angle twist drill. This higher value can be explained due to the construction of the drill itself. However, if the number of cutting edges is considered, in this case, four instead of two, then the average thrust force divided by the number of cutting edges for this drill is approximately equal to the one obtained for the twist 85º or Brad drills, Table 1. The result will be around 45 N for the lower feed rate and 60 to 70 N for the higher feed rate, depending on the drill geometry. In fact, it was already mentioned [4] that an increase in the number of cutting edges combined with a 118º point angle in a twist drill could be a good design in order to minimize the drilling thrust force. This outcome has to be taken into account when observing delamination results or if high productivity is to be considered. So the thrust force and the number of cutting edges can be used for tool comparison and thrust force control, thus allowing increased feed rates when drilling composite laminates.

3.1.2 Feed rate effect

As explained before, the study of feed rate effects was only performed for the two twist drills geometries in this work (120º and 85º point angle twist drills); because according to authors the use of diverse geometries, like Brad or four-flute, could scramble the results. The observed influence of the drill geometry on the thrust force was as expected. Additionally, the effect of feed rate has been previously discussed and

published [7, l0, 11, 14, 24], so this feature could be considered to be validating the experimental work here.

From Figure 9 the effect of the feed rate on thrust force during drilling can be analyzed. Each point of the represented curve represents an average of the holes made with the two drills as indicated for each feed rate. Additionally, in order to enhance the results presented, three feed rates were used to define the curve to show whether the thrust force evolution is linear or exponential. As expected, there is a close relation between the feed rate and the maximum thrust force during drilling. The curve linking the three points is almost linear. Thus, higher feed rates lead to higher thrust force values. This feed rate effect needs to be confirmed by the delamination results, as it is expected that higher thrust forces will result in higher delamination extensions.

3.2 Hole and Delamination Measurements

One of the main goals of the experimental work was the evaluation and comparison of the delamination caused by the drills, through the delamination factor (F_d - Eq. 2) and the adjusted delamination factor (F_{da} - Eq. 3).

The results obtained for the adjusted delamination factor (F_{da}) are indicated in Figure 10 both for drill geometry comparison and feed rate effect. For this comparison, only the two feed rates already mentioned before (0.06 and 0.12 mm/rev) combined with a cutting speed of 53 m/min were considered. The main objective of this comparison is to highlight the importance of drill geometry in delamination extension. Increasing feed rates are known to increase delamination, however the effect of cutting speed was not within the aims of this work. Moreover, different tool materials, such as HSS or PCD, were not included, as their effect could easily interfere with the

conclusions. Other possible options regarding delamination prevention, such as a sacrificial plate or the “front” and “back” clamping with a material of identical or superior stiffness was not considered, as the effect of drill bit would be damped and also some delamination was needed to use the novel image analyses approach developed.

3.2.1 Drill geometry influence

Analyzing the results presented in Figure 10, one can clearly conclude that the use of the 118º angle twist drill gave the lowest delamination values. An identical result was found for the delamination factor (F_d). This outcome is true for both feed rates and is particularly important if we consider issues related to productivity. A 118º twist drill can be used with a feed rate of 0.12 mm/rev with the same or even less delamination extension than was observed with other drill bit geometries using half the feed rate. This result not only indicates that the drill geometry has a strong effect on delamination that cannot be predicted by simple comparison of the thrust forces involved, but also that an adequate choice of drill geometry, for the cutting parameters intended, can help productivity. Thus, this result seems to be of great importance since production cost reductions should always be in the mind of tool manufacturers. The images with the holes produced by the 85º angle twist drills revealed a delamination factor 9% higher than those obtained with the 118º angle twist drill. Delamination caused by the Brad or four flute drills was higher than those caused by the twist drill, Figure 10.

Although the discussion on the influence of feed rate was not seen as a primary objective, it can be concluded that the effect of an increase in the feed rate is not the same with all drills. In fact, for the 118º angle twist drill the delamination was almost unaffected. However, for the other drill geometries, the increase of feed caused a

relevant increase in the delamination factor, the highest difference noted was with the Brad drill.

At this point it should be stated that the tool geometry influence on delamination onset has to be considered, together with the thrust force developed during the drilling operation. That force is different for each tool, under identical cutting parameters and can be mainly related to the drill bit geometry and the chisel edge effect. It is important to remember that a drilling operation is unique, as a consequence of its geometry. The role of the chisel is directly related to the indentation effect, seen as the main cause for delamination [14, 15]. Along the cutting lips, the process cannot be seen as orthogonal cutting but as a three-dimensional oblique cutting process. The cutting speed, the rake angle as well as other variables vary along the cutting lips with the radial distance to the centre. Moreover, at the outer regions of the cutting lips, the cutting action becomes more efficient.

However, the plate properties play an important role in the phenomena of delamination occurrence, due to ply orientation, material stiffness and Young modulus, as demonstrated by known analytical models, see Eq. 1. In all these models, the critical thrust force is only a function of laminate properties and uncut plate thickness. The role of the drill bit geometry and parameter selection is the reduction of the thrust force during drilling.

Another possible cause for the results obtained is the lack of parameter optimization. A selection of cutting parameters for each different drill is needed in order to maximize the tool life together with low quantities of rejections due to delamination damage.

3.2.2 Feed rate effect

The effect of the feed rate in delamination is well evidenced by the values presented in Table 2, representing an average of the results obtained with the two twist drill geometries, differing only in the adopted point angle, for the three feed rates. An increase in delamination is evident when the feed rate is higher. When in comparison with thrust force influence, the outcome is identical: higher feed rates correspond to higher thrust force and delamination, which is in accordance with previous studies, see [8, 18, 24, 25, 26, 36].

From this point of view, a reduction in the feed rate will lead to a reduction in the delamination damage. Nevertheless, this reduction is undesirable if high productivity is expected, so manufacturers should search for an adequate compromise between unavoidable damage, demand for production rates and tool life when designing and recommending parameters for composite material machining.

Once again, it is important to remember that the objective of this work was not only related to the influence of parameters on delamination, but also with the use and validation of a novel computational approach of image segmentation and analysis able to cope with delamination extension measurements from radiographic images. From this point of view, the use of the new approach did not bring any awkward results, which was considered an excellent outcome for this work.

4 Conclusions

In this work, the drilling of carbon/epoxy laminates using four drill geometries and different feed rates was carried out. In order to compare and analyze the experimental delamination damage associated to the drill geometries considered, the thrust forces

involved in the drilling were monitored in runtime and the delamination damage areas were evaluated from radiography images by using a novel approach of image analysis based on an artificial neural network to perform the image segmentation task. Finally, two delamination criterions were used to define the most adequate drilling tool geometry among those used in this work, based on the minimum delamination damage caused. From the analyses of the results obtained, it is possible to draw some important conclusions:

The careful selection of a tool to drill fibre reinforced laminates can be useful. Selection of appropriate drill bit geometry, combined with a correct choice of cutting parameters, will reduce the delamination around the drilled hole. This reduction is not only correlated with the thrust force effect, but also with the drill geometry, as was demonstrated by the experimental results presented. The use of a twist drill with a 118º point angle turned out good results in terms of delamination minimization, although the thrust force was not the lowest one.

The damage around the hole, normally delamination between inner plies of the laminate, can be evaluated by non-destructive testing like the one considered in this work. In fact, the use of suitable techniques for image processing and analysis, in particular the use of the artificial neural network to segment the radiographic images acquired, proved to be adequate to analyze all image areas involved in a very reliable and efficient way, despite the high complexity of the images analyzed.

The techniques for image processing and analysis adopted here were integrated in a novel computational system that was able to identify and quantify the damaged areas caused by drilling in composite materials, mainly associated with the delamination process, as well as the hole area, from radiography images. Additional advantages that

were observed by using the developed computational system are its ease of use, efficiency, accuracy and its robustness to noise that are common in radiographic images. In fact, the novel computational system proposed here can be used for other kinds of materials, composites or not, as well as for different drilling or trimming processes, including laser or abrasive water jetting. Future work will include the application of this system to different cutting processes or materials.

Another possible option for a future comparative work is the use of HSS drills or PCD drills. According to authors' previous experience, the former class of drills leads to extensive damage and the later class returns good results with almost no delamination, but this should be properly evaluated and compared in a future work.

Acknowledgments

The work presented was partially done in the scope of the research projects with references POSC/EEA-SRI/55386/2004 and PTDC/EME-TME/66207/2006, supported by the Portuguese Fundação para a Ciência e a Tecnologia (FCT).

The authors would like to express their deep gratitude to David Graham Straker for her valuable help in reviewing the English version of this paper.

References

1. Wern, C. W., Ramulu, M. and Shukla, A. (1996). Investigation of stresses in the orthogonal cutting of fiber-reinforced plastics, *Experimental Mechanics*, 36(1): 33-41.
2. Abrate, S. (1997). Machining of Composite Materials *Composites Engineering Handbook* (New York, P. K. Mallick, Marcel Dekker).

3. Persson, E., Eriksson, I. and Zackrisson, L. (1997). Effects of hole machining defects on strength and fatigue life of composite laminates, *Composites Part A: Applied Science and Manufacturing*, 28(2): 141-152.

4. Piquet, R., Ferret, B., Lachaud, F. and Swider, P. (2000). Experimental analysis of drilling damage in thin carbon/epoxy plate using special drills, *Composites Part A: Applied Science and Manufacturing*, 31(10): 1107-1115.

5. Palanikumar, K., Rubio, J. C., Abrão, A. M., Correia, A. E. and Davim, J. P. (2008). Influence of Drill Point Angle in High Speed Drilling of Glass Fiber Reinforced Plastics, *Journal of Composite Materials*, 42(24): 2585-2597.

6. Persson, E., Eriksson, I. and Hammersberg, P. (1997). Propagation of Hole Machining Defects in Pin-Loaded Composite Laminates *Journal of Composite Materials*, 31(4): 383-408.

7. Dharan, C. K. H. and Won, M. S. (2000). Machining parameters for an intelligent machining system for composite laminates, *International Journal of Machine Tools and Manufacture*, 40(3): 415-426.

8. Hocheng, H., Puw, H. and Yao, K. (1992). Experimental aspects of drilling of some fibre reinforced plastics *Proceedings of the machining of composite materials symposium - ASM Materials week,* pp. 127-138.

9. Murphy, C., Byrne, G. and Gilchrist, M. D. (2002). The performance of coated tungsten carbide drills when machining carbon-fibre reinforced epoxy composite materials, *Journal of Engineering Manufacture,* 216(2): 143-152.

10. Won, M. and Dharan, C. K. H. (2002). Drilling of aramid and carbon fibre polymer composites, *Journal of Manufacturing Science and Engineering*, 124: 778-783.

11. Won, M. S. and Dharan, C. K. H. (2002). Chisel edge and pilot hole effects in drilling composite laminates, *Journal of Manufacturing Science and Engineering*, 124(2): 242-247.

12. Tsao, C. C. and Hocheng, H. (2003). The effect of chisel length and associated pilot hole on delamination when drilling composite materials, *International Journal of Machine Tools and Manufacture*, 43(11): 1087-1092.

13. Tsao, C. C. (2006). The effect of pilot hole on delamination when core drill drilling composite materials, *International journal of machine tools & manufacture*, 46(12-13): 1653-1661.

14. Durão, L. M., Magalhães, A. G., Tavares, J. M. R. S. and Marques, A. T. (2008). Analyzing objects in images for estimating the delamination influence on load carrying capacity of composite laminates, *Electronic Letters on Computer Vision and Image Analysis*, 7(2): 11-21.

15. Marques, A. T., Durão, L. M., Magalhães, A. G., Silva, J. F. and Tavares, J. M. R. S. (2009). Delamination Analysis of Carbon Fibre Reinforced Laminates: Evaluation of a Special Step Drill, *Composites Science and Technology (DOI: 10.1016/j.compscitech.2009.01.025, in press).*

16. Hocheng, H. and Dharan, C. K. H. (1990). Delamination during drilling in composite laminates, *Journal of Engineering for Industry*, 112: 236-239.

17. Lachaud, F., Piquet, R., Collombet, F. and Surcin, L. (2001). Drilling of composite structures, *Composite Structures*, 52(3): 511-516.

18. Tsao, C. C. and Chen, W. C. (1997). Prediction of the location of delamination in the drilling of composite laminates, *Journal of materials processing technology*, 70(1-3): 185-189.

19. Zhang, L. B., Wang, L. J. and Liu, X. Y. (2001). A mechanical model for predicting critical thrust forces in drilling composite laminates *Proceedings of the Institution of Mechanical Engineers - Part B*, 215(2): 135-146.

20. Tsao, C. C. and Hocheng, H. (2005). Effect of eccentricity of twist drill and candle stick drill on delamination in drilling composite materials, *International journal of machine tools & manufacture*, 45(2): 125-130.

21. Tsao, C. C. and Hocheng, H. (2004). Taguchi analysis of delamination associated with various drill bits in drilling of composite material, *International journal of machine tools & manufacture*, 44(10): 1085-1090.

22. Jung, J. P., Kim, G. W. and Lee, K. Y. (2005). Critical thrust force at delamination propagation during drilling of angle-ply laminates, *Composite Structures*, 68(4): 391-397.

23. Kaynak, C., Akgul, E. and Isitman, N. A. (2008). Effects of RTM Mold Temperature and Vacuum on the Mechanical Properties of Epoxy/Glass Fiber Composite Plates, *Journal of Composite Materials*, 42: 1505-1521.

24. Hosur, M. V., Chowdhury, F. and Jeelani, S. (2007). Low-Velocity Impact Response and Ultrasonic NDE of Woven Carbon/ Epoxy - Nanoclay Nanocomposites, *Journal of Composite Materials*, 41: 2195-2212.

25. Jong, H. J. (2006). Transverse Cracking in a Cross-ply Composite Laminate - Detection in Acoustic Emission and Source Characterization, *Journal of Composite Materials*, 40: 37-69.

26. Johnson, W. S., Treasurer, P. and Woodruff, G. W. (2008). Radiographic Investigation of the Effects of Ply Modification on Damage Development in Laminates Containing Circular Holes, *Journal of Composite Materials*, 42(20): 2143-2161.

27. Rubio, J. C. C., Abrão, A. M., Faria, P. E., Correia, A. E. and Davim, J. P. (2008). Delamination in High Speed Drilling of Carbon Fiber Reinforced Plastic (CFRP), *Journal of Composite Materials*, 42(15): 1523-1532.

28. Chen, W. C. (1997). Some experimental investigations in the drilling of carbon fiber-reinforced plastic (CFRP) composite laminates, *International journal of machine tools & manufacture*, 37(8): 1097-1108.

29. Davim, J. P., Rubio, J. C. and Abrao, A. M. (2007). A novel approach based on digital image analysis to evaluate the delamination factor after drilling composite laminates *Composites Science and Technology*, 67(9): 1939-1945.

30. Tavares, J. M. R. S., Carvalho, F. J. S., Oliveira, F. P. M. et al. Computer Analysis of Objects' Movement in Image Sequences: Methods and Applications *DSM 2007 - Conferência Nacional de Dinâmica de Sistemas Multicorpo*, pp. 33-40 (Portugal).

31. Gonzalez, R. C. and Woods., R. E. (2008). *Digital Image Processing* (USA, Addison Wesley Publishing Company).

32. Ma, Z., Tavares, J. M. R. S., Jorge, R. N. and Mascarenhas, T. (2009). A Review of Algorithms for Medical Image Segmentation and their Applications to the Female Pelvic Cavity, *Computer Methods in Biomechanics and Biomedical Engineering (DOI: 10.1080/10255840903131878, in press)*.

33. Albuquerque, V. H. C., Alexandria, A. R., Cortez, P. C. and Tavares, J. M. R. S. (2009). Evaluation of Multilayer Perceptron and Self-Organizing Map Neural Network Topologies applied on Microstructure Segmentation from Metallographic Images, *NDT & E International*, 42(7): 644-651.

34. Albuquerque, V. H. C., Cortez, P. C., Alexandria, A. R. and Tavares, J. M. R. S. (2008). A New Solution for Automatic Microstructures Analysis from Images

Based on a Backpropagation Artificial Neural Network, *Nondestructive Testing and Evaluation*, 23(4): 273-283.

35. Gonçalves, P. C. T., Tavares, J. M. R. S. and Jorge, R. M. N. (2008). Segmentation and Simulation of Objects Represented in Images using Physical Principles, *Computer Modeling in Engineering & Sciences*, 32(1): 45-55.

36. Vasconcelos, M. J. M. and Tavares, J. M. R. S. (2008). Methods to Automatically Built Point Distribution Models for Objects like Hand Palms and Faces Represented in Images, *Computer Modeling in Engineering & Sciences*, 36(2): 213-241.

37. Tavares, J. M. R. S. (2000). PhD Thesis: Analysis of the Movement of Deformable Bodies using Computational Vision (in Portuguese) (University of Porto, Portugal).

38. Bhadeshia, H. K. D. H. (2006). *Neural networks and genetic algorithms in materials science and engineering* (India, Tata McGraw-Hill Publishing Company Ltd.).

39. Miaoquan, L., Liu, X., Xiong, A. and Li, X. (2002). An adaptive prediction model of grain size for the forging of Ti-6Al-4V alloy based on the fuzzy neural networks, *Journal of materials processing technology*, 123(3): 377-381.

40. Miaoquan, L., Liu, X., Xiong, A. and Li, X. (2003). Microstructural evolution and modelling of the hot compression of a TC6 titanium alloy *Materials Characterization*, 49(3): 203-209.

41. Kim, I., Jeong, Y., Lee, C. and Yarlagadda., P. (2003). Prediction of welding parameters for pipeline welding using an intelligent system, *The International Journal of Advanced Manufacturing Technology*, 22(9): 713-719.

42. Kusiak, J. and Kusiak, R. (2002). Modelling of microstructure and mechanical properties of steel using the artificial neural network *Journal of materials processing technology*, 127(1): 115-121.

43. Li, X. and Miaoquan, L. (2005). Microstructure evolution model based on deformation mechanism of titanium alloy in hot forming *Transactions of non ferrous metals society of China*, 15(4): 749-753.

44. Biernacki, R., Kozłowski, J., Myszka, D. and Perzyk, M. (2006). Prediction of properties of austempered ductile iron assisted by artificial neural network, *Materials Science (Medžiagotyra)*, 12(1): 11-15.

45. Abdelhay, A. (2002). Application of artificial neural networks to predict the carbon content and the grain size for carbon steels, *Egyptian Journal of Solids*, 25(2): 229-243.

46. Wang, O., Lai, J. and Sun, D. (2007). Artificial neural network models for predicting flow stress and microstructure evolution of a hydrogenized titanium alloy, *Key Engineering Materials*, 353: 541-544.

47. Zhang, G. P. (2000). Neural networks for classification: A survey, *IEEE Transactions on Systems, Man and Cybernetics - Part C: Applications and reviewers*, 30(4): 451-462.

48. Samarasinghe, S. (2006). *Neural networks for applied sciences and engineering: from fundamentals to complex pattern recognition* (USA, Auerbach Publications).

49. Haykin, S. (1994). *Neural networks: a comprehensive foundation* (USA, Macmillian College Publishing Company Inc).

50. Yin, X. C., Liu, C. P. and Han, Z. (2005). Feature combination using boosting,

Pattern Recognition Letters, 25(14): 2195-2205.

FIGURE CAPTIONS

Figure 1: Delamination mechanisms: a) peel-up; b) push-down.

Figure 2: Topology of the artificial neural network used.

Figure 3: Block diagram of the experimental work performed.

Figure 4: Experimental setup used.

Figure 5: Drills used: a) twist 118º; b) twist 85º; b) Brad; c) four-flute.

Figure 6: Examples of radiographies acquired from the drilled plates using the: a) twist 118º; b) twist 85º; b) Brad; c) four-flute.

Figure 7: Example of a delamination damage characterization from a radiographic image: a) original image; b) segmented image; c) delamination area; d) drilled hole area.

Figure 8: Influence of drill geometry and feed rate on thrust force.

Figure 9: Effect of feed rate on thrust force during drilling.

Figure 10: Influence of drill geometry and feed rate on adjusted delamination factor (F_{da}).

TABLE CAPTIONS

Table 1. Summary of the experimental results for maximum thrust force per cutting edge (C.E) and delamination factors.

Table 2. Measured average effects of the feed rate considering two twist drills (of 118º and 85º).

FIGURES

Figure 1a

Figure 1b

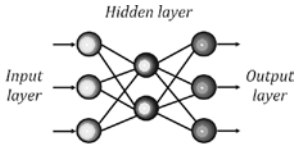

Figure 2

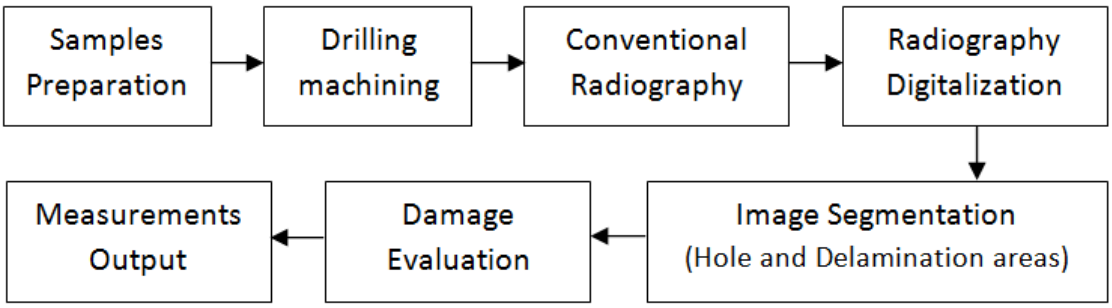

Figure 3

Figure 4

Figure 5a

Figure 5b

Figure 5c

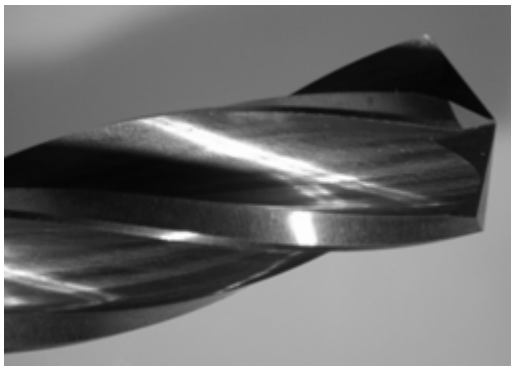

Figure 5d

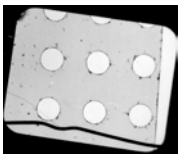

Figure 6a

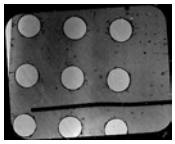

Figure 6b

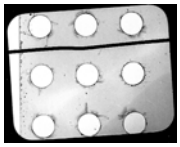

Figure 6c

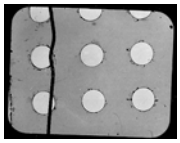

Figure 6d

Figure 7a

Figure 7b

Figure 7c

Figure 7d

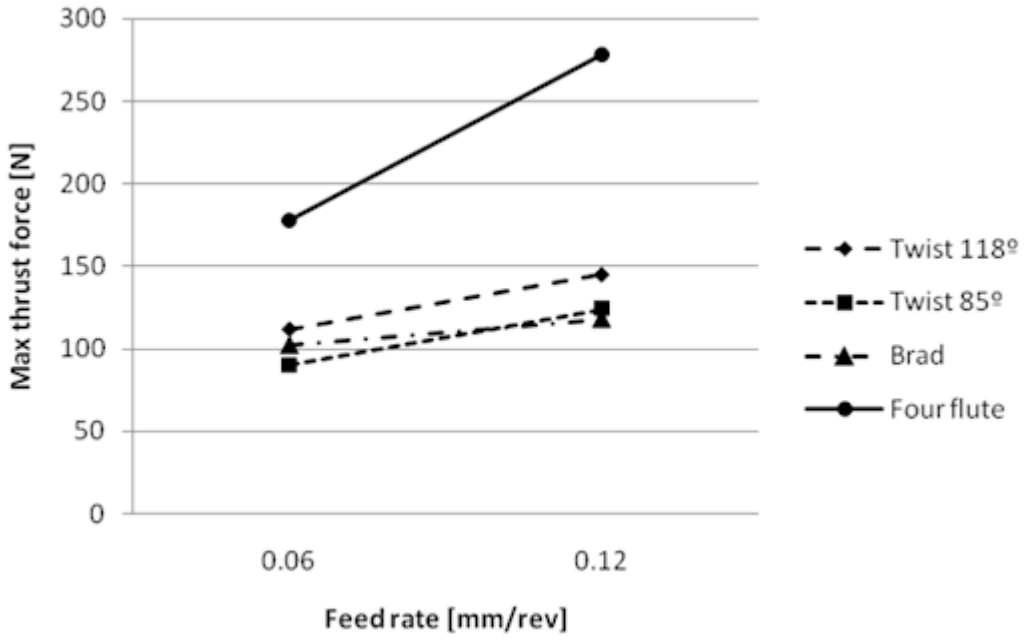

Figure 8

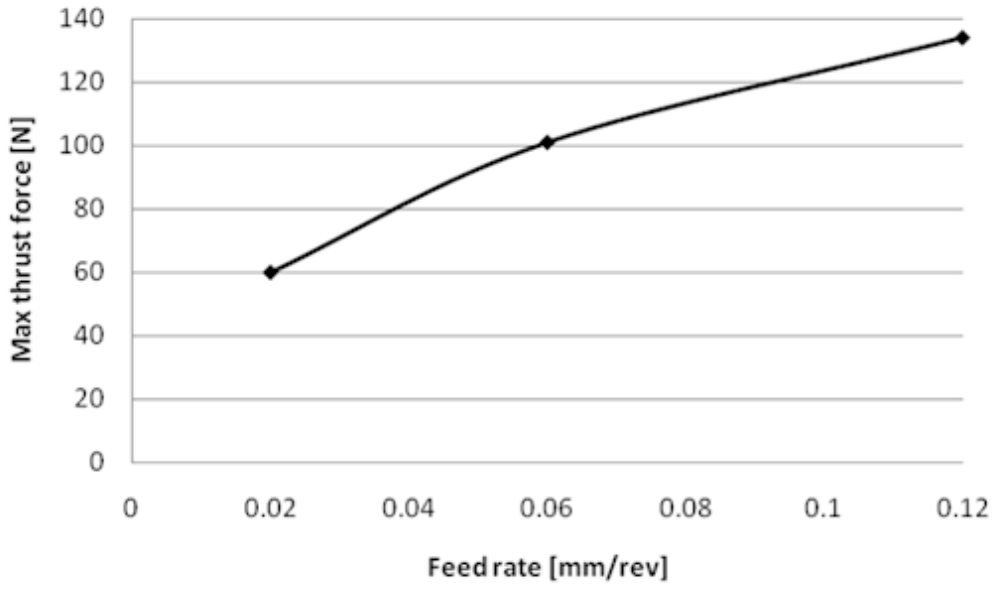

Figure 9

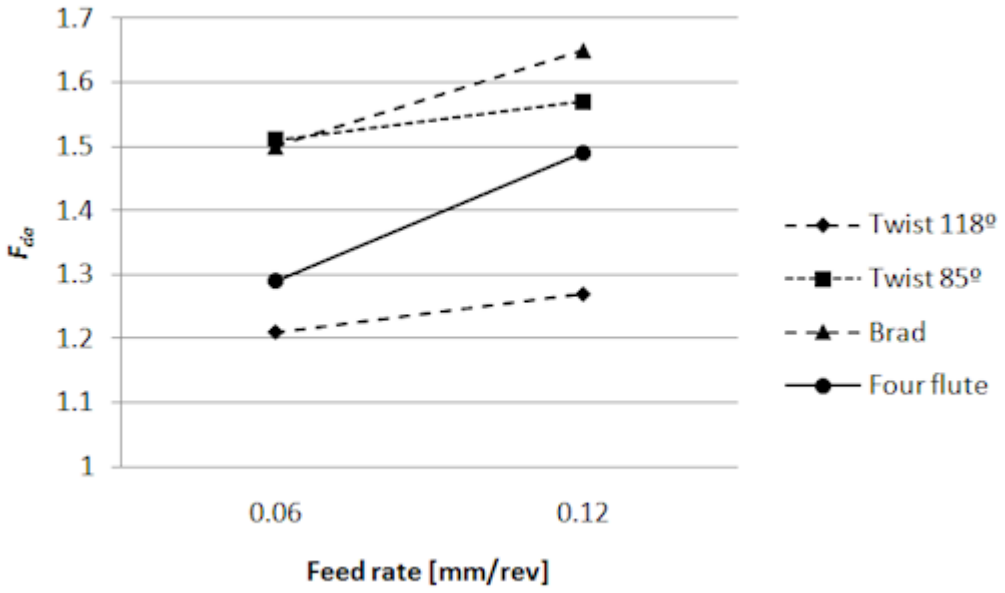
1.7
1.6
1.5
1.4
1.3
1.2
1.1
1
F_{da}
0.06
0.12
Feed rate [mm/rev]
Twist 118º
Twist 85º
Brad
Four flute

Figure 10

TABLES

Table 1

Drill	Max. thrust force per C. E. [N]		Delamination factor (F_d)		Adjusted delamination factor (F_{da})	
Twist 120º (2 C. E.)	56	73	1.15	1.19	1.21	1.27
Twist 85º (2 C. E.)	45	62	1.40	1.42	1.51	1.57
Brad (2 C. E.)	51	59	1.33	1.44	1.50	1.65
Four flute (4 C. E.)	45	70	1.21	1.28	1.29	1.49
Feed rate [mm/rev]	0.06	0.12	0.06	0.12	0.06	0.12

Table 2

Feed rate [mm/rev]	Max. thrust force [N]	Delamination Factor (F_d)	Adjusted delamination factor (F_{da})
0.02	60	1.12	1.30
0.06	101	1.27	1.36
0.12	134	1.31	1.42